J|A|C|S
ARTICLES
Published on Web 03/03/2007

Effect of Elemental Composition of PtPd Bimetallic Nanoparticles Containing an Average of 180 Atoms on the Kinetics of the Electrochemical Oxygen Reduction Reaction

Heechang Ye and Richard M. Crooks*

Contribution from the Department of Chemistry and Biochemistry, Texas Materials Institute, Center for Nano and Molecular Science and Technology, The University of Texas at Austin, 1 University Station A5300, Austin, Texas 78712-0165

Received November 11, 2006; E-mail: crooks@cm.utexas.edu

Abstract: PtPd bimetallic nanoparticles containing an average of 180 atoms and composed of seven different Pt:Pd ratios have been prepared within sixth-generation, hydroxyl-terminated, poly(amidoamine) dendrimers. Transmission electron microscopy indicates that the sizes of all seven nanoparticle compositions are within ±0.2 nm of one another and the calculated size. Single-particle energy-dispersive spectroscopy shows that the elemental composition is determined by the ratio of the Pt and Pd precursor salts used to prepare the nanoparticles. Cyclic voltammetry and rotating disk voltammetry measurements show that the Pt:Pd ratio of the nanoparticles determines their efficiency for the oxygen reduction reaction (ORR). The maximum activity for the ORR occurs at a Pt:Pd ratio of 5:1, which corresponds to a relative mass activity enhancement of 2.4 compared to otherwise identical monometallic Pt nanoparticles.

Introduction

In this paper, we demonstrate that well-defined PtPd bimetallic catalysts prepared by dendrimer templating can be used to precisely correlate the effect of catalyst composition to the efficiency of the oxygen reduction reaction (ORR) (Scheme 1). This is a significant finding for two reasons. First, dendrimer templating is the only method we are aware of for preparing very well defined, electrocatalytically active bimetallic nanoparticles in the <3 nm size range. Here, "well defined" means size distributions having standard deviations of ±0.3 nm and particle-to-particle elemental compositional variations of ≤7%. Second, dendrimer-encapsulated catalysts can be characterized prior to electrode immobilization using, for example, methods like transmission electron microscopy (TEM) and single-particle energy-dispersive spectroscopy (EDS). This ensures that catalytic performance is not dominated by a small number of unique particles, which in turn makes it possible to directly correlate the elemental composition of the particles to their catalytic function. The results of this study indicate that certain bimetallic compositions of Pt and Pd exhibit more favorable kinetics for the ORR than particles of identical size but composed exclusively of Pt.

Dendrimer-encapsulated nanoparticles (DENs) are prepared in two-steps.[1] First, metal ions are extracted into dendrimers and coordinate in fixed stoichiometries with interior functional groups. Second, the intradendrimer metal ions are reduced to yield DENs. This process leads to stable, nearly size-monodisperse, catalytically active nanoparticles composed of Pt,[2−7] Pd,[2,5,6,8−18] Au,[19−22] or Cu.[23] It is also possible to prepare alloy[24−27] and core/shell[26,27] bimetallic DENs using a slight variation of this basic approach. Monometallic and bimetallic DENs have previously been shown to be catalytically active for homogeneous hydrogenation and carbon−carbon coupling reactions[28] as well as for heterogeneous catalytic reactions.[29,30]

Scheme 1

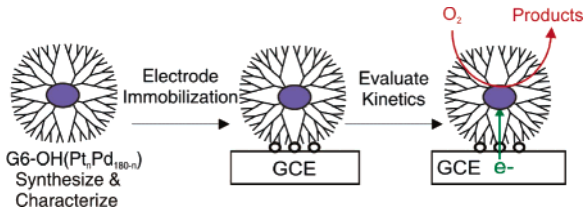

(1) Scott, R. W. J.; Wilson, O. M.; Crooks, R. M. *J. Phys. Chem. B* **2005**, *109*, 692−704, and references therein.
(2) Zhao, M.; Crooks, R. M. *Angew. Chem., Int. Ed.* **1999**, *38*, 364−366.
(3) Zhao, M.; Crooks, R. M. *Adv. Mater.* **1999**, *11*, 217−220.
(4) Esumi, K.; Nakamura, R.; Suzuki, A.; Torigoe, K. *Langmuir* **2000**, *16*, 7842−7846.
(5) Oh, S.-K.; Kim, Y.-G.; Ye, H.; Crooks, R. M. *Langmuir* **2003**, *19*, 10420−10425.
(6) Ye, H.; Scott, R. W. J.; Crooks, R. M. *Langmuir* **2004**, *20*, 2915−2920.
(7) Ye, H.; Crooks, R. M. *J. Am. Chem. Soc.* **2005**, *127*, 4930−4934.
(8) Niu, Y.; Yeung, L. K.; Crooks, R. M. *J. Am. Chem. Soc.* **2001**, *123*, 6840−6846.
(9) Niu, Y.; Crooks, R. M. *Chem. Mater.* **2003**, *15*, 3463−3467.
(10) Scott, R. W. J.; Ye, H.; Henriquez, R. R.; Crooks, R. M. *Chem. Mater.* **2003**, *15*, 3873−3878.
(11) Chechik, V.; Zhao, M.; Crooks, R. M. *J. Am. Chem. Soc.* **1999**, *121*, 4910−4911.
(12) Chechik, V.; Crooks, R. M. *J. Am. Chem. Soc.* **2000**, *122*, 1243−1244.
(13) Yeung, L. K.; Crooks, R. M. *Nano Lett.* **2001**, *1*, 14−17.
(14) Yeung, L. K.; Lee, C. T., Jr.; Johnston, K. P.; Crooks, R. M. *Chem. Commun.* **2001**, 2290−2291.
(15) Li, Y.; El-Sayed, M. A. *J. Phys. Chem. B* **2001**, *105*, 8938−8943.
(16) Ooe, M.; Murata, M.; Mizugaki, T.; Ebitani, K.; Kaneda, K. *Nano Lett.* **2002**, *2*, 999−1002.
(17) Garcia-Martinez, J. C.; Lezutekong, R.; Crooks, R. M. *J. Am. Chem. Soc.* **2005**, *127*, 5097−5103.
(18) Wilson, O. M.; Knecht, M. R.; Garcia-Martinez, J. C.; Crooks, R. M. *J. Am. Chem. Soc.* **2006**, *128*, 4510−4511.
(19) Kim, Y.-G.; Oh, S.-K.; Crooks, R. M. *Chem. Mater.* **2004**, *16*, 167−172.

Finally, we recently reported that Pt-only monometallic DENs can be immobilized on glassy carbon electrodes and that the resulting DEN monolayers are stable and electrocatalytically active for the ORR.[7]

At present, Pt is the most common ORR catalyst. However, there have been numerous recent studies of the effect of multimetallic catalysts on the ORR. For example, the performances of bulk-alloy electrodes[31−33] and thin-film alloys[34−36] have been evaluated. However, improvements in ORR activity have been most commonly associated with nanophase multimetallic alloys containing Pt, such as Pt−Co,[37−41] Pt−Ni,[37,38,42] Pt−Cr,[37,43] and Pt−Fe,[39,40,44] supported on carbon electrodes. Zhang et al. reported a particularly interesting approach for preparing structured nanophase catalysts via deposition of catalytically active metals over a nonnoble core.[45] These materials, as well as related nonparticulate thin films,[46,47] possess very high mass activities for the ORR. There have also been recent efforts to eliminate Pt from ORR catalysts altogether, and many materials have been reported that have ORR activities approximating that of Pt.[48−50] Finally, theoretical studies have appeared that provide insight into the origin of the activity enhancements in multimetallic ORR catalysts.[40,47,51−54]

In this paper, we report the synthesis of well-defined bimetallic PtPd electrocatalysts containing an average of 180 total atoms (∼1.8 nm in diameter) but seven different ratios of Pt:Pd. TEM and EDS indicate that individual nanoparticles having particular Pt:Pd ratios are remarkably uniform in size and composition. Following complete characterization, these catalysts were immobilized onto the surface of a glassy carbon electrode and their effectiveness was evaluated as a function of composition using cyclic voltammetry and rotating disk voltammetry. The results indicate that PtPd bimetallic DENs of most compositions enhance the catalytic activity of the ORR. The maximum relative mass activity enhancement of 240% (vs the equivalent monometallic Pt DEN catalyst) occurs for bimetallic nanoparticles containing 17−33% Pd.

Experimental Section

Chemicals. Sixth-generation, hydroxyl-terminated, poly(amidoamine) dendrimers (G6-OH) were purchased as an 11.46% methanol solution (Dendritech, Inc., Midland, MI). Prior to use, the methanol was removed under vacuum. K_2PdCl_4 (Strem Chemicals, Inc., Newburyport, MA), K_2PtCl_4, $NaBH_4$, $LiClO_4$ (Sigma-Aldrich, Inc.), and H_2SO_4 (J.T.Baker, Ultrex II) were used without further purification. To prepare aqueous solutions, 18 MΩ·cm Milli-Q deionized water (Millipore) was used. Research-grade O_2 gas (Praxair, 99.999%) was used for the ORR.

Preparation of PtPd DENs. PtPd DENs were prepared according to a previously published procedure.[24] Briefly, an aqueous solution containing K_2PtCl_4 and K_2PdCl_4 prepared freshly (within 5 min) was added to a 10 μM aqueous G6-OH solution. The final metal-to-dendrimer ratio was fixed at 180:1 and the Pt:Pd ratio was adjusted to n:(180 − n) where n = 180, 150, 120, 90, 60, 30, and 0. The metal complex/dendrimer solution was stirred for 72 h to allow the Pt and Pd ions to fully complex with the interior amines of the dendrimers.[2,3,6] Zerovalent PtPd DENs (G6-OH(Pt_nPd_{180-n})) were produced by slow addition of a 10-fold molar excess of aqueous 0.5 M $NaBH_4$ to this solution. The resulting PtPd DEN solutions were allowed to stand in a closed vial for 24 h to ensure complete reduction. Finally, the solution was dialyzed for 24 h using a cellulose dialysis sack having a molecular weight cutoff of 12 000 (Sigma-Aldrich, Inc.) to remove impurities.[10]

Electrochemistry. Glassy carbon (GC) disks (Pine Instruments, 5.0-mm diameter) were used as electrodes. Glassy carbon electrodes (GCEs) were prepared by successive polishing with 1.0- and 0.3-μm alumina powder on a polishing cloth (Buehler) followed by sonication in water for 5 min. The electrodes were then rinsed with water and were dried under flowing N_2 gas. All electrochemical experiments were performed in a single-compartment glass cell using a standard three-electrode configuration with a Pt-gauze (DEN immobilization) or a Au coil (ORR experiments) counter electrode and a mercury/mercurous sulfate reference electrode (CH Instruments, Inc., Austin, TX). For convenience, measured potentials are reported versus the reversible hydrogen electrode (RHE). Cyclic voltammetry and rotating disk voltammetry were performed using a computer-controlled Pine Instruments (Grove City, PA) AFRDE4 potentiostat and ASR rotator. All electrochemical experiments were performed at 22 ± 1 °C.

Characterization. X-ray photoelectron spectroscopy (XPS) data were acquired using an Axis His 165 Ultra (Kratos, Manchester, United

(20) Gröhn, F.; Bauer, B. J.; Akpalu, Y. A.; Jackson, C. L.; Amis, E. J. *Macromolecules* **2000**, *33*, 6042−6050.
(21) Gröhn, F.; Gu, X.; Grüll, H.; Meredith, J. C.; Nisato, G.; Bauer, B. J.; Karim, A.; Amis, E. J. *Macromolecules* **2002**, *35*, 4852−4854.
(22) Esumi, K.; Satoh, K.; Torigoe, K. *Langmuir* **2001**, *17*, 6860−6864.
(23) Zhao, M.; Sun, L.; Crooks, R. M. *J. Am. Chem. Soc.* **1998**, *120*, 4877−4878.
(24) Scott, R. W. J.; Datye, A. K.; Crooks, R. M. *J. Am. Chem. Soc.* **2003**, *125*, 3708−3709.
(25) Chung, Y.-M.; Rhee, H.-K. *Catal. Lett.* **2003**, *85*, 159−164.
(26) Scott, R. W. J.; Wilson, O. M.; Oh, S.-K.; Kenik, E. A.; Crooks, R. M. *J. Am. Chem. Soc.* **2004**, *126*, 15583−15591.
(27) Wilson, O. M.; Scott, R. W. J.; Garcia-Martinez, J. C.; Crooks, R. M. *J. Am. Chem. Soc.* **2005**, 1015−1024.
(28) Niu, Y.; Crooks, R. M. *C. R. Chimie* **2003**, *6*, 1049−1059.
(29) Lang, H.; May, R. A.; Iversen, B. L.; Chandler, B. D. *J. Am. Chem. Soc.* **2003**, *125*, 14832−14836.
(30) Scott, R. W. J.; Wilson, O. M.; Crooks, R. M. *Chem. Mater.* **2004**, *16*, 5682−5688.
(31) Glass, J. T.; Cahen, G. L., Jr.; Stoner, G. E.; Taylor, E. J. *J. Electrochem. Soc.* **1987**, *134*, 58−65.
(32) Paffett, M. T.; Beery, J. G.; Gottesfeld, S. *J. Electrochem. Soc.* **1988**, *135*, 1431−1436.
(33) Stamenkovic, V.; Schmidt, T. J.; Ross, P. N.; Markovic, N. M. *J. Phys. Chem. B* **2002**, *106*, 11970−11979.
(34) Toda, T.; Igarashi, H.; Uchida, H.; Watanabe, M. *J. Electrochem. Soc.* **1999**, *146*, 3750−3756.
(35) Toda, T.; Igarashi, H.; Watanabe, M. *J. Electroanal. Chem.* **1999**, *460*, 258−262.
(36) Wakabayashi, N.; Takeichi, M.; Uchida, H.; Watanabe, M. *J. Phys. Chem. B* **2005**, *109*, 5836 -5841.
(37) Min, M.-K.; Cho, J.; Cho, K.; Kim, H. *Electrochim. Acta* **2000**, *45*, 4211−4217.
(38) Paulus, U. A.; Wokaun, A.; Scherer, G. G.; Schmidt, T. J.; Stamenkovic, V.; Radmilovic, V.; Markovic, N. M.; Ross, P. N. *J. Phys. Chem. B* **2002**, *106*, 4181−4191.
(39) Murthi, V. S.; Urian, R. C.; Mukerjee, S. *J. Phys. Chem. B* **2004**, *108*, 11011−11023.
(40) Anderson, A. B.; Roques, J.; Mukerjee, S.; Murthi, V. S.; Markovic, N. M.; Stamenkovic, V. *J. Phys. Chem. B* **2005**, *109*, 1198−1203.
(41) Salgado, J. R. C.; Antolini, E.; Gonzalez, E. R. *J. Phys. Chem. B* **2004**, *108*, 17767−17774.
(42) Yang, H.; Vogel, W.; Lamy, C.; Alonso-Vante, N. *J. Phys. Chem. B* **2004**, *108*, 11024−11034.
(43) Yang, H.; Alonso-Vante, N.; Leger, J.-M.; Lamy, C. *J. Phys. Chem. B* **2004**, *108*, 1938−1947.
(44) Hwang, J. T.; Chung, J. S. *Electrochim. Acta* **1993**, *38*, 2715−2723.
(45) Zhang, J.; Lima, F. H. B.; Shao, M. H.; Sasaki, K.; Wang, J. X.; Hanson, J.; Adzic, R. R. *J. Phys. Chem. B* **2005**, *109*, 22701−22704.
(46) Zhang, J.; Mo, Y.; Vukmirovic, M. B.; Klie, R.; Sasaki, K.; Adzic, R. R. *J. Phys. Chem. B* **2004**, *108*, 10955−10964.
(47) Zhang, J.; Vukmirovic, M. B.; Sasaki, K.; Nilekar, A. U.; Mavrikakis, M.; Adzic, R. R. *J. Am. Chem. Soc.* **2005**, *127*, 12480−12481.
(48) Fernández, J. L.; Raghuveer, V.; Manthiram, A.; Bard, A. J. *J. Am. Chem. Soc.* **2005**, *127*, 13100−13101.
(49) Raghuveer, V.; Manthiram, A.; Bard, A. J. *J. Phys. Chem. B* **2005**, *109*, 22909−22912.
(50) Shao, M.-H.; Sasaki, K.; Adzic, R. R. *J. Am. Chem. Soc.* **2006**, *128*, 3526−3527.
(51) Xu, Y.; Ruban, A. V.; Mavrikakis, M. *J. Am. Chem. Soc.* **2004**, *126*, 4717−4725.
(52) Balbuena, P. B.; Altomare, D.; Vadlamani, N.; Bingi, S.; Agapito, L. A.; Seminario, J. M. *J. Phys. Chem. A* **2004**, *108*, 6378−6384.
(53) Wang, Y.; Balbuena, P. B. *J. Phys. Chem. B* **2005**, *109*, 18902−18906.
(54) Nørskov, J. K.; Rossmeisl, J.; Logadottir, A.; Lindqvist, L.; Kitchin, J. R.; Bligaard, T.; Jónsson, H. *J. Phys. Chem. B* **2004**, *108*, 17886−17892.
(55) Leff, D. V.; Ohara, P. C.; Heath, J. R.; Gelbart, W. M. *J. Phys. Chem.* **1995**, *99*, 7036−7041.

Table 1. Measured and Calculated Particle Sizes for Pt, PtPd, and Pd DENs

sample	average particle size	calculated size[a]
G6-OH(Pt_{180})	1.8 ± 0.3 nm	1.73 nm
G6-OH($Pt_{150}Pd_{30}$)	1.7 ± 0.3 nm	
G6-OH($Pt_{120}Pd_{60}$)	1.7 ± 0.3 nm	
G6-OH($Pt_{90}Pd_{90}$)	1.7 ± 0.3 nm	
G6-OH($Pt_{60}Pd_{120}$)	1.7 ± 0.3 nm	
G6-OH($Pt_{30}Pd_{150}$)	1.8 ± 0.3 nm	
G6-OH(Pd_{180})	1.9 ± 0.3 nm	1.72 nm

[a] Calculated using the equation $n = 4\pi r^3/3V_g$, where n is the number of Pt or Pd atoms, r is the radius of the Pt or Pd nanoparticle, and V_g is the volume of one Pt (15.1 Å^3) or Pd (14.7 Å^3) atom calculated from the molar volume.[55]

Table 2. Atomic % Analysis of Individual G6-OH($Pt_{120}Pd_{60}$), G6-OH($Pt_{90}Pd_{90}$), and G6-OH($Pt_{60}Pd_{120}$) DENs

	G6-OH($Pt_{120}Pd_{60}$)		G6-OH($Pt_{90}Pd_{90}$)		G6-OH ($Pt_{60}Pd_{120}$)	
particle	Pt (%)	Pd (%)	Pt (%)	Pd (%)	Pt (%)	Pd (%)
#1	72	28	50	50	36	64
#2	71	29	41	59	43	57
#3	71	29	52	48	38	62
#4	63	37	61	39	40	60
#5	69	31	46	54	41	59
average	69 ± 4	31 ± 4	50 ± 7	50 ± 7	39 ± 3	61 ± 3

Kingdom) with a Mg Kα X-ray source. The XPS positions were referenced to the C(1s) peak at 284.5 eV. Instead of using GC disks, GC plates (Tokai Carbon Co., grade GC-20) were used as electrodes for XPS measurements. TEM and EDS measurements were performed using a JEOL-2010F TEM configured with an Oxford INCA energy-dispersive spectrometer. Samples were prepared by placing several drops of solution on a carbon-coated Cu TEM grid and allowing the solvent to evaporate in air.

Results and Discussion

Characterization of Bimetallic DENs. Seven different G6-OH(Pt_nPd_{180-n}) (n = 180, 150, 120, 90, 60, 30, and 0) DENs were synthesized and then characterized by TEM to determine their average size and size distribution (Supporting Information and Table 1). Assuming a spherical geometry, the calculated diameter of G6-OH(Pt_nPd_{180-n}) DENs is 1.7 nm. The average measured diameters for the seven different compositions used in this study ranged from 1.7 to 1.9 nm.

Previously, we found that the molar ratio of metal salts or complexes (in this case, K_2PdCl_4 and K_2PtCl_4) used to prepare bimetallic DENs is reflected in the nanoparticle composition after reduction.[24,26] To confirm that this is true in the present case, single-particle EDS analysis was performed for three of the DEN composition: (G6-OH($Pt_{120}Pd_{60}$), G6-OH($Pt_{90}Pd_{90}$), and G6-OH($Pt_{60}Pd_{120}$). Five particles selected randomly from each of these compositions were analyzed, and the results are provided in Table 2. Additionally, the Supporting Information provides a typical single-particle EDS spectrum for G6-OH($Pt_{90}Pd_{90}$). The EDS results indicate that the measured Pt:Pd ratios agree very well with the anticipated values (in parentheses) on the basis of the ratios of the metal complexes used for the synthesis: G6-OH($Pt_{120}Pd_{60}$), 2.2 (2.0); G6-OH($Pt_{90}Pd_{90}$), 1.0 (1.0); and G6-OH($Pt_{60}Pd_{120}$), 0.6 (0.5). On the basis of the average compositions and sizes of the PtPd DENs, and the modest particle-to-particle variations in size and composition, we conclude that the O_2 reduction kinetics discussed later can be directly correlated to the composition of the DENs. That is, the electrochemical results are unlikely to be dominated by small populations of particles having unanticipated sizes or compositions. Indeed, the ability to correlate a population of particles having uniform structures to their catalytic function is the main point of this study.

Immobilization of Pt and PtPd DENs on GCEs. The immobilization of Pt and PtPd DENs on GCEs was carried out using a previously published procedure.[7] Briefly, a freshly polished GCE was placed in an aqueous 10 μM Pt or PtPd DEN solution containing 0.1 M $LiClO_4$, and then the electrode potential was scanned three times between 0.50 and 1.40 V (vs RHE) at a scan rate of 10 mV/s. Next, the electrode was rinsed with water, sonicated in water for 5 min, dried under flowing N_2 gas, and then immediately placed in the electrolyte solution used for ORR experiments. We have previously shown that this procedure results in robust immobilization of the dendrimer and that the DENs are in electrical communication with the electrode surface.[7] We have also demonstrated that the nanoparticles are retained within the dendrimers following electrode immobilization.[7] To confirm that the electrode coverage of DENs is independent of the type of encapsulated metal, we carried out the following experiment. An equimolar mixture of G6-OH(Pt_{180}) and G6-OH(Pd_{180}) DENs was immobilized on a GCE using the just-described electrochemical anchoring method, and then the elemental composition of the electrode surface was evaluated by XPS (Supporting Information, Figure S4). The resulting XPS spectrum revealed that the atomic percentages of Pt and Pd on the surface were the same, indicating that the identity of the encapsulated nanoparticle does not bias the surface composition of DENs. We have previously shown that dendrimers adsorb onto surfaces at a constant number density that depends only on the generation of the dendrimer.[56] We infer from that study that the catalytic results reported next are not influenced by differences in the surface concentration of DENs.

Cyclic Voltammetry. Electrodes modified with seven different types of DENs (G6-OH(Pt_nPd_{180-n}), n = 180, 150, 120, 90, 60, 30, and 0) were prepared as described in the previous section, and their electrocatalytic properties were qualitatively evaluated using cyclic voltammetry. Figure 1a shows a series of seven cyclic voltammograms (CVs) obtained using electrodes modified with DENs having the same average number of atoms but different Pt:Pd ratios. All CVs were acquired in an O_2-saturated aqueous electrolyte solution containing 0.5 M H_2SO_4 and using a scan rate of 50 mV/s. Before the CVs were obtained, the electrodes were activated by scanning the potential between 0.95 and 0 V two times in the same electrolyte solution. Each CV (except G6-OH(Pd_{180})) exhibits a well-defined peak between 0.70 and 0.55 V that corresponds to the ORR. For example, the peak current for the electrode modified with G6-OH(Pt_{180}) is found at 0.67 V, but the electrodes coated with bimetallic PtPd DENs having low percentages of Pd exhibit ORR peaks at more positive potentials (e.g., 0.70 and 0.68 V for G6-OH($Pt_{150}Pd_{30}$) and G6-OH($Pt_{120}Pd_{60}$), respectively). This suggests that these bimetallic PtPd DENs have enhanced electrocatalytic ORR activity. Figure 1b summarizes the CV data by showing the potential of the peak current for the ORR as a function of increasing Pt percentage in each electrocatalytic

(56) Tokuhisa, H.; Zhao, M.; Baker, L. A.; Phan, V. T.; Dermody, D. L.; Garcia, M. E.; Peez, R. F.; Crooks, R. M.; Mayer, T. M. *J. Am. Chem. Soc.* **1998**, *120*, 4492−4501.

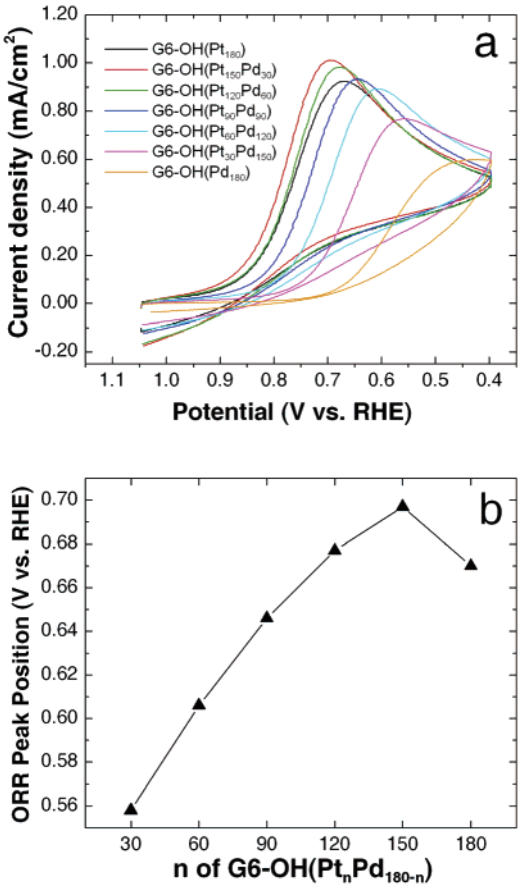

Figure 1. (a) Cyclic voltammograms of G6-OH(Pt_nPd_{180-n})(n = 180, 150, 120, 90, 60, 30, and 0). (b) A plot of the peak current position for the ORR as function of n of G6-OH(Pt_nPd_{180-n}). Scan rate: 50 mV/s; electrolyte solution: aqueous 0.5 M H_2SO_4 saturated with O_2.

particle. From these data, it is clear that the maximum catalytic activity is achieved for G6-OH($Pt_{150}Pd_{30}$).

For electrocatalytic reactions, it is important to know the active surface area of the catalyst. We determined this value experimentally using the hydrogen adsorption/desorption method.[57,58] Figure 2 shows CVs of G6-OH(Pt_nPd_{180-n}) (n = 180, 150, 120, and 90) and a voltammogram obtained using an electrode modified with G6-OH only (no metal particles). CVs of DEN-modified electrodes exhibit broad peaks between 0.05 and 0.3 V that are characteristic of hydrogen adsorption and desorption. Small shoulders characteristic of hydrogen adsorption on bulk Pt[57] are only just noticeable in the CV of G6-OH(Pt_{180}), but as the Pd content increases, these features are lost and the total charge associated with hydrogen increases slightly. These latter two changes probably arise from differences in adsorption characteristics of hydrogen on the bimetallic surface and possibly because of some insertion of hydrogen into the interior of the Pd-containing bimetallics (absorption). Additionally, the total charge associated with the hydrogen adsorption/desorption region of the CVs decreases significantly during continuous voltammetric scanning for PtPd DENs containing more than 60 atoms of Pd. We calculated the active surface area of the stable G6-OH(Pt_{180}) catalyst on the basis of the charge associated with the hydrogen desorption region (anodic

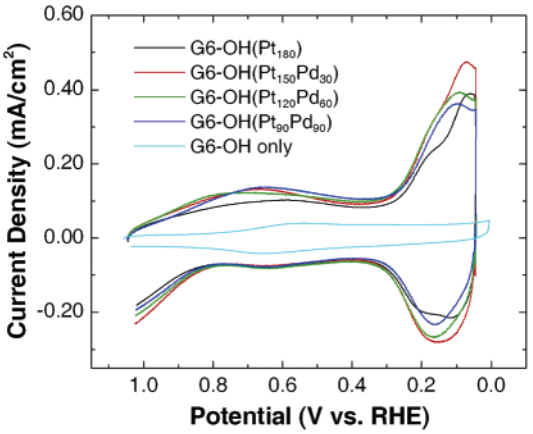

Figure 2. Cyclic voltammograms of G6-OH(Pt_nPd_{180-n})(n = 180, 150, 120, and 90) in N_2-saturated, 0.5 M H_2SO_4 electrolyte solution. A cyclic voltammogram of an electrode modified only with G6-OH is also shown. Scan rate: 100 mV/s. The initial potential was 1.05 V.

current between 0.05 and 0.3 V). After subtraction of the background charge, the total charge was 46 μC, which corresponds to 0.22 cm^2 of active surface area assuming that hydrogen desorption yields 210 $\mu C/cm^2$ of Pt surface area.[57]

It is also possible to estimate the surface area of the Pt and PtPd DENs with a simple calculation and appropriate assumptions. We have previously shown that dendrimers form near-monolayer coverages on most surfaces.[56] Thus, assuming monolayer coverage, a projected area for each dendrimer of 35 nm^2, that one nanoparticle is encapsulated within each dendrimer, that each nanoparticle is a sphere having a diameter of 1.8 nm, and that the roughness factor of GC surfaces is 2.4, which is an average value from the literature (range: 1.3−3.5),[59−61] a total metal surface area of 0.14 cm^2 can be calculated for G6-OH(Pt_{180}) on the 5-mm-diameter GCE. This value is in reasonable agreement with the experimentally determined value obtained by hydrogen desorption for G6-OH(Pt_{180}) of 0.22 cm^2. The mass of Pt corresponding to the total Pt surface area of 0.14 cm^2 is 0.088 μg or 0.45 $\mu g/cm^2$ when normalized to the projected surface area of the electrode.

Rotating Disk Voltammetry. The electrocatalytic activity of PtPd DENs was quantitatively examined as a function of catalyst composition using rotating disk voltammetry.[33,38,62,63] The rotating disk electrodes (RDEs) were modified with DENs following the same procedure used for the CV experiments. Figure 3a shows a family of rotating disk voltammograms (RDVs) for the G6-OH(Pt_{180}) electrocatalyst obtained at rotation rates ranging from 200 to 2500 rpm. These RDVs were measured using electrolyte solutions having the same composition as that used for the CVs, and the potential was scanned from 0.95 to 0.15 V at 10 mV/s. Figure 3a only shows the forward-going scan, but a comparison of the forward and reverse scans is provided in the Supporting Information (Figure S5). The amount of hysteresis is about 45 mV, which is typical for all the RDVs described here.

The RDVs in Figure 3a exhibit onset currents at about 0.80 V and attain mass-transfer-limited values that are a function of

(57) Biegler, T.; Rand, D. A. J.; Woods, R. *J. Electroanal. Chem.* **1971**, *29*, 269−277.
(58) Pozio, A.; De Francesco, M.; Cemmi, A.; Cardellini, F.; Giorgi, L. *J. Power Sources* **2002**, *105*, 13−19.
(59) Rice, R. J.; McCreery, R. L. *Anal. Chem.* **1988**, *61*, 1637−1641.
(60) Pontikos, N. M.; McCreery, R. L. *J. Electroanal. Chem.* **1992**, *324*, 229−242.
(61) Lee, C.-W.; Bard, A. J. *J. Electroanal. Chem.* **1988**, *239*, 441−446.
(62) Schmidt, T. J.; Gasteiger, H. A.; Stab, G. D.; Urban, P. M.; Kolb, D. M.; Behm, R. J. *J. Electrochem. Soc.* **1998**, *145*, 2354−2358.
(63) Gasteiger, H. A.; Kocha, S. S.; Sompalli, B.; Wagner, F. T. *Appl. Catal., B* **2005**, *56*, 9−35.

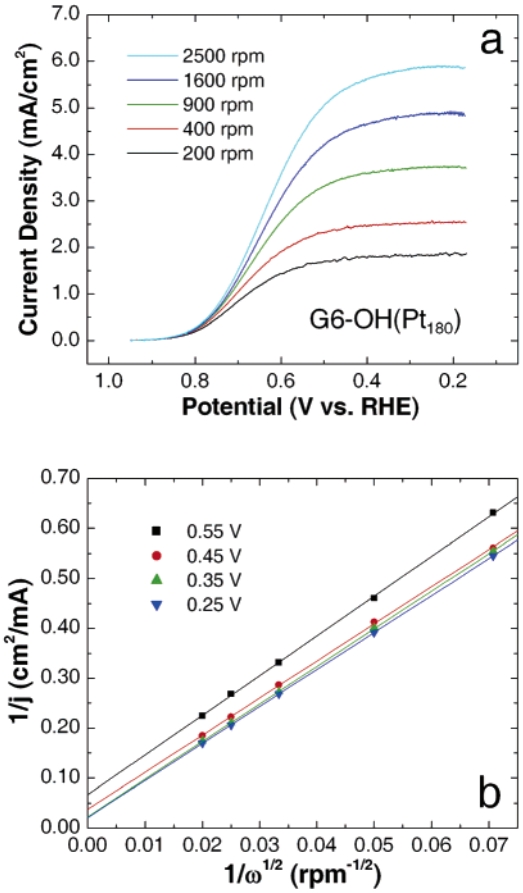

Figure 3. (a) Rotating disk voltammograms for a G6-OH(Pt_{180})-modified GCE. (b) Plots of $1/j$ vs $1/\omega^{1/2}$ derived from the RDVs in a. Scan rate: 10 mV/s; electrolyte solution: aqueous 0.5 M H_2SO_4 saturated with O_2.

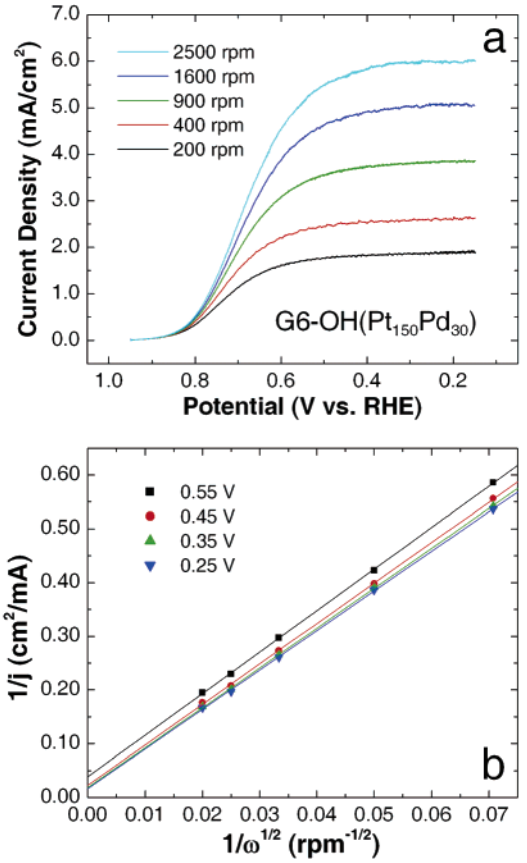

Figure 4. (a) Rotating disk voltammograms for a G6-OH($Pt_{150}Pd_{30}$)-modified GCE. (b) Plots of $1/j$ vs $1/\omega^{1/2}$ derived from the RDVs in a. Scan rate: 10 mV/s; electrolyte solution: aqueous 0.5 M H_2SO_4 saturated with O_2.

the rotation rate. The observed current is attributable to O_2 reduction, because no measurable current was observed when a N_2-saturated electrolyte solution was scanned in this same potential window. The G6-OH($Pt_{150}Pd_{30}$)-modified RDE shows slightly different results (Figure 4a). The shapes of the voltammograms are the same as in Figure 3a, but the RDVs are shifted to a more positive potential. For example, the RDV obtained at 900 rpm for the G6-OH(Pt_{180}) catalyst attains a current density of 2.0 mA/cm^2 at 0.64 V while the G6-OH($Pt_{150}Pd_{30}$) catalyst exhibits this same current density at 0.69 V. This means that the G6-OH($Pt_{150}Pd_{30}$) DENs are more active ORR catalysts than the G6-OH(Pt_{180}) DENs. The potentials of the RDVs are reproducible (±10 mV) for independently synthesized G6-OH(Pt_{180}) and G6-OH($Pt_{150}Pd_{30}$) electrocatalysts immobilized on independently prepared electrodes. As the percentage of Pd in the DEN electrocatalysts increases, the RDVs retain a similar appearance, except that they shift to more negative potentials compared to G6-OH($Pt_{150}Pd_{30}$), indicating that they have inferior catalytic properties. These additional RDVs are provided in the Supporting Information. Importantly, the CVs and RDVs provide consistent information: maximum catalytic activity is observed for G6-OH($Pt_{150}Pd_{30}$), and as the percentage of Pd increases, the catalytic performance monotonically decreases.

Figures 3b and 4b are Koutecky−Levich plots[64] ($1/j$ vs $1/\omega^{1/2}$) as a function of potential for the G6-OH(Pt_{180}) and G6-OH($Pt_{150}Pd_{30}$) DENs, respectively. We compared the slopes of these Koutecky−Levich plots with the theoretically calculated values for the four-electron O_2 reduction using eq 1.

$$\frac{1}{j} = \frac{1}{j_K} + \frac{1}{j_d} = \frac{1}{j_K} + \frac{1}{0.20nFD_O^{2/3}\omega^{1/2}\nu^{-1/6}C_O} = \frac{1}{j_K} + \frac{1}{B\omega^{1/2}} \quad (1)$$

Here, j is the measured current density, j_K is the kinetic current density, j_d is the diffusion (mass-transfer) limited current density, F is the Faraday constant, D_O is the diffusion coefficient of O_2 (1.9×10^{-5} cm^2/s), ω is electrode rotation rate in unit of rpm, ν is kinematic viscosity of water (1.0×10^{-2} cm^2/s), and C_O is the concentration of O_2 in dilute, aqueous sulfuric acid (1.1×10^{-6} mol/cm^3).[65,66] Using appropriate numerical values, the calculated B value is 0.13 mA/cm^2-rpm$^{1/2}$. This value can be compared to the measured B values obtained from the slopes of the plots in Figures 3b and 4b of 0.132 ± 0.004 mA/cm^2-rpm$^{1/2}$ and 0.133 ± 0.003 mA/cm^2-rpm$^{1/2}$ for the G6-OH(Pt_{180}) and G6-OH($Pt_{150}Pd_{30}$) DENs, respectively. The excellent agreement between the calculated and measured B values means that the number of electrons involved in the ORR with these DEN catalysts is four, and thus the predominant product is water. The Koutecky−Levich plots for G6-OH($Pt_{120}Pd_{60}$), G6-OH($Pt_{90}Pd_{90}$), and G6-OH($Pt_{60}Pd_{120}$) have B values of 0.135 ± 0.004

(64) Bard, A. J.; Faulkner, L. R. *Electrochemical Methods Fundamentals and Application*, 2nd ed.; John Wiley & Sons: New York, 2001; pp 340−344.

(65) Gubbins, K. E.; Robert, D. Walker, J. *J. Electrochem. Soc.* **1965**, *112*, 469−471.

(66) *CRC Handbook of Chemistry and Physics*, Internet Version 2006; Lide, D. R., Ed.; Taylor and Francis: Boca Raton, FL, 2006; http://www.hbcpnetbase.com.

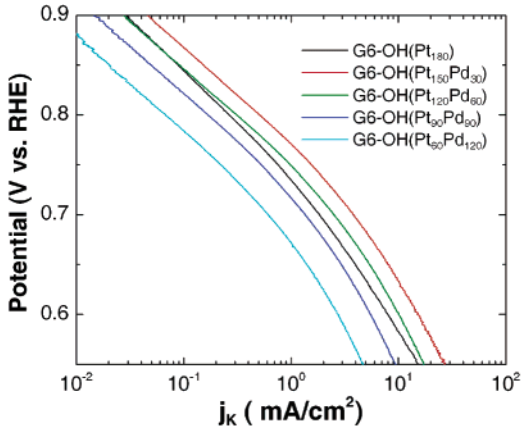

Figure 5. Tafel plots for Pt and PtPd catalysts obtained using data from RDVs (900 rpm).

Table 3. Tafel Slopes for the ORR Using Pt and PtPd DEN Electrocatalysts Measured at Low and High Overpotentials[a]

	Tafel slope (V/decade)	
sample	(>0.75 V)	(<0.70 V)
G6-OH(Pt_{180})	−0.106/−0.105	−0.157/−0.153
G6-OH($Pt_{150}Pd_{30}$)	−0.098/−0.096	−0.164/−0.167
G6-OH($Pt_{120}Pd_{60}$)	−0.095/−0.087	−0.166/−0.166
G6-OH($Pt_{90}Pd_{90}$)	−0.097/−0.095	−0.164/−0.167
G6-OH($Pt_{60}Pd_{120}$)	−0.097	−0.160

[a] Data for two independently synthesized and tested DEN catalysts are shown for all but G6-OH($Pt_{60}Pt_{120}$).

mA/cm^2-rpm$^{1/2}$, 0.131 ± 0.005 mA/cm^2-rpm$^{1/2}$, and 0.133 ± 0.004 mA/cm^2-rpm$^{1/2}$ and are provided in the Supporting Information (Figure S6).

A kinetic analysis for the Pt and PtPd electrocatalysts, determined using the RDVs described previously, was carried out using Tafel plots. Specifically, Figure 5 shows plots of potential versus kinetic current density (j_K), where the j_K values were obtained from the j and j_d values of the RDVs (900 rpm) in Figures 3a, 4a, and S6 (Supporting Information) using eq 1.[63,67,68] As is commonly observed for the ORR, the Tafel plots in Figure 5 exhibit two distinct slopes at low (>0.75 V) and high (<0.70 V) overpotential (Table 3). Within these two potential regions, the slopes and shapes of the Tafel plots for all the bimetallic compositions are nearly identical, suggesting the ORR mechanism is the same for all of them. However, the shape of the Tafel plot for the G6-OH(Pt_{180}) catalyst is slightly different, which might indicate that the presence of Pd affects the ORR mechanism. The Tafel slopes (Table 3) are higher than those for other Pt and Pt-based bimetallic catalysts reported in the literature.[33,38,46,69] The underlying reason for this is beyond the scope of our present study, but as our work in this area evolves, we hope to be able to quantitatively address questions like this. Finally, we obtained Tafel plots derived from RDVs scanned in the opposite direction from those in Figure 3 (Figure S7). These plots have almost the same shape and slope as those shown in Figure 5, but they are shifted positive by about 45 mV.

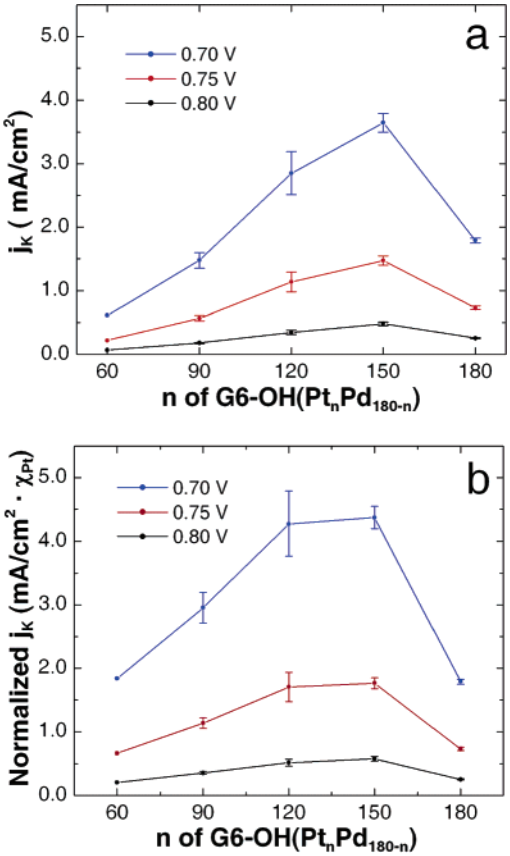

Figure 6. Plots of (a) kinetic current density and (b) kinetic current density normalized to the fractional amount of Pt contained in each nanoparticle composition at different potentials. Error bars represent the span of data for two independently executed experiments (only one experiment was carried out for G6-OH($Pt_{60}Pd_{120}$).

Figure 6a shows a comparison of kinetic data for G6-OH(Pt_nPd_{180-n}) obtained from Figure 5 at different potentials. As for the CV results (Figure 1), the kinetic current density increases in G6-OH($Pt_{150}Pd_{30}$) compared to G6-OH(Pt_{180}) but as the Pd content increases further the current density decreases.

The data in Figure 6b were obtained by dividing j_K (Figure 6a) by the fraction of Pt used in the DEN synthesis (e.g., 0.5 for G6-OH($Pt_{90}Pd_{90}$)). This makes it possible to compare the relative mass activity of Pt in the PtPd DEN catalysts. The relative mass activity is the same as the relative specific activity if all catalysts are random alloys and are the same size. For this value to have meaning, it is necessary to assume that Pd does not exhibit measurable catalytic activity in the relevant potential range (0.70−0.80 V, Figure 6). The voltammetry of G6-OH(Pd_{180}) shown in Figure 1a confirms this assumption. The key result is that for the data at 0.70 V, there is an enhancement in relative mass activity of ∼2.4 for the G6-OH($Pt_{150}Pd_{30}$) and G6-OH($Pt_{120}Pd_{60}$) electrocatalysts compared to G6-OH(Pt_{180}).

Finally, we estimated the specific activity (kinetic current normalized to the total surface area of catalyst) and the mass activity (kinetic current normalized to the total mass of catalyst) for G6-OH(Pt_{180}) at 0.70 V on the basis of the total surface area and mass of Pt discussed earlier. The estimated specific activity for G6-OH(Pt_{180}) ranges from 1.6 to 2.5 mA/cm$_{Pt}^2$, depending on whether the experimentally measured surface area (0.22 cm^2) or the calculated value (0.14 cm^2) is used. The

(67) Maciá, M. D.; Campiña, J. M.; Herrero, E.; Feliu, J. M. *J. Electroanal. Chem.* **2004**, *564*, 141−150.
(68) Sode, A.; Li, W.; Yang, Y.; Wong, P. C.; Gyenge, E.; Mitchell, K. A. R.; Bizzotto, D. *J. Phys. Chem. B* **2006**, *110*, 8715−8722.
(69) Paulus, U. A.; Schmidt, T. J.; Gasteiger, H. A.; Behm, R. J. *J. Electroanal. Chem.* **2001**, *495*, 134−145.

estimated mass activity for G6-OH(Pt_{180}) is 4.0 mA/μg_{Pt} on the basis of the calculated mass of Pt present on the electrode surface (0.088 μg).

Summary and Conclusions

We have examined the catalytic activity of DENs containing 180 atoms and composed of seven different Pt:Pd ratios. The most important conclusion of this paper is that multimetallic nanoparticles having very well defined compositions can be synthesized and structurally and chemically characterized ex situ, and then these properties can be directly correlated to their electrocatalytic activity. This provides a direct and reproducible means for correlating the structure and function of electrocatalysts. Eventually, it might be possible to use this approach to develop experimental models that are sufficiently well-defined to test first-principles calculations.

Cyclic and rotating disk voltammetry results indicate that PtPd bimetallic DENs exhibit relative mass activity enhancements for the ORR of up to a factor of 2.4 compared to monometallic Pt DENs. However, the Pt and PtPd DEN catalysts presented in this paper require 50−100 mV of additional overpotential compared to commercial carbon-supported Pt catalysts in other ORR kinetic studies.[38,63,69] This could be the result of different experimental conditions, such as temperature, electrolyte composition, and hysteresis in the voltammetry. Alternatively, or in addition, there could be a particle-size effect that suppresses catalytic activity: the catalysts used in this study were composed of ~1.7 nm particles, but others have reported that the optimal size for the ORR is in the range of 3−4 nm.[63,70,71] Finally, if our model is correct (Scheme 1), there could be an overpotential required for electron tunneling between the electrode and the catalytic nanoparticles or because of the presence of N ligands from the dendrimer adsorbed to the nanoparticle surface. It is important to keep in mind, however, that the G6-OH(Pt_{180}) catalyst films reported here consist of single monolayers containing a total Pt loading of 0.45 $\mu g/cm^2$. This amount corresponds to 30−100 times less metal per unit electrode area compared to most prior studies.[38,42,43,63,69] To compare Pt DEN activity to a known standard, we obtained rotating disk voltammograms using a bulk Pt electrode. Of course, all experimental conditions were the same as for the DEN experiments. The results indicate that the overpotential for the ORR is about 80 mV less for bulk Pt compared to a G6-OH(Pt_{180})-modified GCE electrode. The likely reasons for this difference have already been discussed.

At present, we are examining the effect of the size of Pt-only DENs on the activity of the ORR. Subsequent electrocatalytic studies will focus on other types of multimetallic DENs in both alloy and core−shell forms.

Acknowledgment. We gratefully acknowledge the U.S. Department of Energy, DOE-BES Catalysis Science grant no. DE-FG02-03ER15471, and the National Science Foundation (Grant No. 0531030) for financial support of this project. We also acknowledge SPRING and the Robert A. Welch Foundation for support of some of the instrumentation used in this project. We thank Yulia Vasilyeva of the Texas A&M University Materials Characterization Facility for assistance in obtaining the XPS data and Dr. Ji-Ping Zhou of the Texas Materials Institute at UT-Austin for help with the TEM and EDS measurements.

Supporting Information Available: TEM images and particle-size distribution for the G6-OH(Pt_nPd_{180-n}) (n = 180, 150, 120, 90, 60, and 30); single-particle EDS spectrum of G6-OH(Pt_{90}-Pd_{90}); XPS spectrum of a DEN monolayer prepared from a physical mixture of G6-OH(Pt_{180}) and G6-OH(Pd_{180}); an RDV showing both the negative and positive potential scans; RDVs and Koutecky−Levich plots for G6-OH($Pt_{120}Pd_{60}$), G6-OH(Pt_{90}-Pd_{90}), and G6-OH($Pt_{60}Pd_{120}$) DENs; comparison of Tafel plots as a function of scan directions; comparison of RDVs obtained using a bulk Pt electrode and a G6-OH(Pt_{180})-modified GCE. This material is available free of charge via the Internet at http://pubs.acs.org.

JA068078O

(70) Kinoshita, K. *J. Electrochem. Soc.* **1990**, *137*, 845−848.
(71) Mayrhofer, K. J. J.; Blizanac, B. B.; Arenz, M.; Statenkovic, V. R.; Ross, P. N.; Markovic, N. M. *J. Phys. Chem. B* **2005**, *109*, 14433−14440.